Supporting Information for

Cyanobacterial dihydroxyacid dehydratases are a promising growth inhibition target

Peilan Zhang, Brian S. MacTavish, Guang Yang, Manyun Chen, Jaehyeok Roh, Kevin R. Newsome, Steven D. Bruner, Yousong Ding

Corresponding authors: Steven D. Bruner and Yousong Ding

Email: bruner@chem.ufl.edu; yding@cop.ufl.edu

This PDF file includes:

Materials and general methods

General methods

Molecular biology reagents and chemicals were purchased from Thermo Scientific, NEB, Fisher Scientific or Sigma-Aldrich. GeneJET Plasmid Miniprep Kit and GeneJETGel Extraction Kit (Thermo Scientific) were used for plasmid preparation and DNA purification, respectively. All oligonucleotide primers used were ordered from Sigma-Aldrich while DNA sequencing was performed at Eurofins. Aspterric acid was purchased from Cayman Chemical. *E. coli* BL21 (DE3) (Agilent) was used for routine molecular biology studies and protein expression and was grown in Luria-Bertani broth or Terrific broth. All microbial strains were purchased from commercial sources (**Table S2**). Cyanobacteria were cultured in BG-11 medium (Sigma-Aldrich) at 26 °C. The cultures were air bubbled and received a lighting cycle of 16 h/8 h (light/dark) with the illumination of 2000–2500 lux.

Molecular cloning, protein expression and purification

The genes encoding dihydroxyacid dehydratase in *Synechocystis* sp. PCC 6803 (GenBank: BA000022.2:3498903-3500588) and *E. coli* K-12 (Gene ID: 948277) were amplified from corresponding isolated genomic DNAs with a pair of primers SnFw and SnRv or EcFw and EcRv (**Table S3**). Amplicons were cloned into pET28a to give *N*-His_6 tagged products. The resultant pET28a-SnDHAD construct was also used as the template to create SnDHAD mutants (C50S, C123S, S437A, D124L, D124E, Y477H, and Y477T) by site-directed mutagenesis PCR with primers shown in **Table S3**. The inserts were sequenced to exclude any potential errors introduced during PCR reactions. All expression constructs were transformed in *E. coli* BL21 (DE3) to produce recombinant proteins. Protein expression was carried out in TB medium supplemented with 50 μg/mL kanamycin. The cells were grown at 37 °C, 250 rpm until OD_{600} reached 0.6. L-Cysteine (final concentration 1 mM), $(NH_4)_2Fe(SO_4)_2$ (final concentration 2 mM), and IPTG (final concentration 0.1 mM) were then added to the culture to induce gene expression at 18°C, 250 rpm for 20 h. The cells were harvested by centrifugation (6,000 x *g*, 10 min). The collected cell pellets were then resuspended in lysis buffer (50 mM Tris-Cl, pH 8, 100 mM NaCl, 1 mM DTT and 10 mM imidazole) and were sonicated to release soluble proteins. Following centrifugation (20,000 x *g*, 4 °C, 45 min), recombinant DHAD proteins were purified from clear, cell-free supernatants with HisPur Ni-NTA Resin (Thermo Fisher Scientific) according to the manufacturer's protocol, along with washing buffer (50 mM Tris-Cl, pH 8, 100 mM NaCl, 1 mM DTT and 30 mM imidazole) and elution buffer (50 mM Tris-Cl, pH 8, 100 mM NaCl, 1 mM DTT and 200 mM imidazole). The final desalting was attained by buffer exchange into storage buffer (50 mM Tris-Cl, pH 8, 1 mM DTT) with a PD-10 column (GE Healthcare Life Science). Purified DHAD proteins were further concentrated (Amicon® Ultra-15, 10 k MWCO) to 10.0 $mg \cdot mL^{-1}$ for further analysis. Protein concentrations were determined with Bradford assay (BSA as standard).

Quantification of iron content in recombinant DHADs

The iron content in recombinant DHADs were quantitated by the ferrozine assay.[1] Briefly, protein samples (100 μL) and 0.01 M ferrozine (10 μL) were mixed well in flat-bottom microplate. Next, 20 μL of 1.4 M hydroxylamine hydrochloride solution were added to the above mixtures and the resultant solutions were incubated at room temperature for 10 min to completely reduce Fe(III). Subsequently, 20 μL of 10 M ammonium acetate solution were added to the above solution and mixed thoroughly. The mixtures were then centrifuged at 5,000 x *g*, 20 °C for 10 min to remove insoluble debris and 100 μL of the supernatant were transferred to a clear 96-well flat plate to record the absorbance at 562 nm with a microplate reader (BioTek). A linear, standard curve was pre-established with $FeCl_3$ (10 mM stock solution) in the range of 0 to 0.32 mM. The Fe contents of proteins

were calculated from the standard curve. The storage buffer (50 mM Tris-Cl, pH 8, 1 mM DTT) was used as a negative control. All experiments were independently repeated at least three times.

Characterization of enzyme activity

The reaction solutions (100 μL) of EcDHAD, SnDHAD and its mutants (C50S, C123S, S437A, D124L, D124E and Y477H) contained 50 mM Tris-Cl, pH 8.0, 1 mM DTT, 10 mM $MgCl_2$ and 1 mM 2*R*-DHIV. The reactions were initiated by mixing with 0.25 μM of proteins, aerobically incubated at room temperature for 30 min, and then terminated by mixing with 25 μL of 2 M HCl. Enzymatically synthesized KIV in the solutions was then derivatized with 50 μL of saturated 2,4-dinitrophenylhydrazine (DNPH) in 2 M HCl at room temperature for 30 min. Next, 25 μL of 10 M NaOH were added to each reaction solution and mixed well. Centrifugation at 5,000 x *g* for 10 min was followed to remove precipitates. To detect KIV-DNPH adduct, 100 μL of the supernatant were transferred to a clear 96-well flat bottom microplate to record the absorbance at 540 nm. The standard curve of KIV-DNPH adduct showed an excellent linearity in the range of 0-1 mM ($y = 0.001x + 0.006$, $R^2 = 0.9915$; $y = OD_{540}$, x = [KIV]). To detect KIV-DNPH adduct by LC-MS analysis, the pH of reaction mixture was adjusted to neutral. AB Sciex 3200 QTRAP spectrometer coupled with a Shimadzu Prominence HPLC system was used. The compound was separated on Agilent Poroshell 120 Phenyl Hexyl column (2.7 μm, 3.0 mm × 50 mm) with a 10 min linear gradient from 5 to 95% acetonitrile in 0.1% formic acid at a flow rate of 0.8 mL/min. The product was detected at 380 nm and in negative mode of MS. For MS detection, the turbo spray conditions were: curtain gas: 20 psi; ion spray voltage: 5000 V; temperature: 500 °C; ion source gas 1: 30 psi; ion source gas 2: 40 psi. Ions were detected in the negative mode.

To evaluate the relative catalytic activities of SnDHAD and its mutants, the catalytic reactions contain 0.25 μM of enzymes and were conducted under room temperature for 30 min. The oxygen stabilities of SnDHAD and EcDAHD were characterized by exposing the enzyme solutions (1.25 μM) to air at 4 ºC and room temperature for up to two weeks. At designed time points, 20 μL of enzyme solutions were collected to determine residual catalytic activity in the reaction described above. To determine the optimal pH for the SnDHAD reaction, the reactions described above were performed in citric acid–sodium citrate buffer, Na_2HPO_4-NaH_2PO_4 buffer and Na_2CO_3-$NaHCO_3$ buffer, which together covered a pH range of 3 to 10. To determine the optimal temperature, the reactions were incubated at 4, 25, 37, 50, 65, 80 and 100 °C for 30 min. The thermostability of SnDHAD was evaluated by pre-treating the protein solution at certain temperatures (37, 50, 65, and 80 °C) for 15, 30, 60 and 120 min before measuring the residual activity using above described method. To characterize metal dependency, recombinant SnDHAD was incubated with 0, 1, and 10 mM of cation solutions ($CaCl_2$, $CoCl_2$, $CuCl_2$, $FeCl_2$, $MgCl_2$, $MnCl_2$, $ZnCl_2$, $NiCl_2$, and NaCl) and EDTA at room temperature for 15 min and then performed activity measurement in the above reaction mixture without 10 mM $MgCl_2$. To assess the potential inhibition activity of tartronic acid and aspterric acid, the reactions of recombinant SnDHAD were included with serial concentrations of these chemicals. For the kinetic study, the reaction mixtures contained 0.05 μM as-purified SnDHAD and serial concentrations of DHIV (0, 50, 100, 200, 400, 600, 800, 1000 μM) and incubated for 30 min at room temperature. The inhibition effect on SnDHAD was measured using different concentrations of aspterric acid and tartronic acid. The inhibition percentage was calculated as (1 – amount of KIV with inhibitor/ amount of KIV without inhibitor) × 100%. All enzyme activities were determined in triplicate.

Genetic complementation of *E. coli* Δ*ilvD* with transiently expressed SnDHAD

The *E. coli* Δ*ilvD* mutant was created by modifying a previously established Scarless Cas9 Assisted Recombineering (no-SCAR) method.[2] Briefly, we created psgRNA-ilvD using primers listed in **Table S3**, and transformed it along with pCas9-CR4 plasmids (Addgene #62655) into *E. coli* BL21(DE3). The transformed strain was then cultured in LB medium supplemented with 50 μg/mL spectinomycin and 25 μg/mL chloramphenicol until reaching OD_{600} of 0.4 at 30 °C. Next, arabinose (1.2% final concentration) was added to induce the expression of λ-Red recombinase for 15 min prior to the collection of cells for preparing electrocompetent cells. We then amplified one kanamycin resistance cassette from pUC4K using Km-Fw and Km-Rv (**Table S3**) that carried immediate upstream and downstream homologous regions of *ilvD*, respectively. After purification, 500 ng of amplicons were used to transform above *E. coli* BL21(DE3) electrocompetent cells. After recovering at 30 °C for 1 h, the cells were plated on LB agar supplemented with 50 μg/mL kanamycin and anhydrotetracycline to induce the genome editing system. The positive transformants were screened in PCR reactions to amplify the edited region in the genomes and the amplicons were further verified by DNA sequencing. Finally, the *E. coli* Δ*ilvD* mutant was treated to cure psgRNA-ilvD and pCas9-CR4 plasmids.[2] The full genotype of the mutant is *E. coli* F^- *omp*T *hsd*S_B (rB^-, mB^-) *gal dcm* Δ*ilvD* (DE3). This mutant was then used to prepare electrocompetent cells for transformation with pSnDHAD, which was constructed by cloning *SnDHAD* into pET22b using primers listed in **Table S3**. The positive transformats were selected on LB agar media supplemented with 50 μg/mL kanamycin and 100 μg/mL ampicillin. The complementation test was initiated by incubating the positive transformants in M9 minimum medium supplemented with either three BCAAs (1 mM each) or IPTG (0.1 mM). The wild type *E. coli* BL21(DE3) was served as the control. The activity of the transiently expressed SnDHAD in *E. coli* Δ*ilvD* mutant was assessed by monitoring cell growth (OD_{600}) every hour for up to 8 hours. To further validate the catalytic function of the transiently expressed SnDHAD, 50 mM tartronate were included in the complementation tests. All experiments were independently performed in triplicate.

Crystallization and structure determination of SnDHAD

SnDHAD was expressed and purified via nickel NTA affinity chromatography as described above. Additional chromatography steps of anion-exchange (Mono Q) and Gel Filtration (S200) were applied before concentration to 20 mg/mL. Crystallization trials were performed using the sitting drop vapor diffusion method with a variety of commercial screens and positive crystal hits were observed from the Hampton Index screen (condition 83: 0.2 M Mg_2Cl-hexahydrate, 0.1 M Bis-Tris pH 6.5, 25 % PEG 3,350) to yield crystals with a platelet morphology with dimensions of ~10 μm x 10 μm. Diffraction data sets were collected at LS-CAT, 21-ID-F beamline, Advanced Proton Source, Argonne National Laboratory at a wavelength of 0.9786 angstroms (MARMOSAIC225 detector, 100K). Native data sets were processed using the XDS software package.[3] SnDHAD crystals diffracted to 2.34 Å in the P21 space group with two molecules per unit cell. The phase solution was determined by molecular replacement using the apo 6-phosphogluconate dehydratase structure from *Shewanella oneidensis* (PDB: 2GP4) as the model. Model building was performed using Chainsaw,[4] BUCCANEER,[5] and Phenix refine.[6] Calculated R_{work} and R_{free} for the final model were 0.172/0.224, respectively. Relevant data collection, phasing, and refinement statistics may be found in **Table S4**. The atomic coordinates and structure factors have been deposited in the Protein Data Bank under the ID code 6NTE.

Modeling missing loops and docked substrates into SnDHAD

The final structure of SnDHAD contained a substantial missing loop (a.a. 155-195) and two additional loops represented by poor electron density (a.a. 44-54 and 80-88). A total of 61 amino acids over these three loops were built with RosettaCM[7] using D-xylonate

dehydratase (PDB: 5OYN) and L-arabinonate dehydratase (PDB: 5J84) as templates. Alignment of these three structures was performed using Clustal Omega.[8] Using the best model from RosettaCM, the [2Fe-2S] cluster and Mg^{2+} from AtDHAD (PDB: 5ZE4) and DHIV were manually placed into the active site of SnDHAD. The complex holo structure was minimized and relaxed using RosettaScripts[9] with the geometry constraints of [2Fe-2S] cluster cysteine bonds.

Phylogenetic analysis of DHADs

DHAD protein sequences from model organisms were obtained by protein BLAST search against the NCBI landmark database (E-value <1e−5) using query sequences for known DHAD: *E. coli* DHAD (Sequence ID: WP_094888139.1), *Mycobacterium tuberculosis* DHAD (Sequence ID: WP_003900824.1), *Sulfolobus acidocaldarius* DHAD (WP_011278523.1), *Synechocystis* DHAD (Sequence ID: WP_010874288.1) and *Candida albicans* DHAD (Sequence ID: XP_721948.1). After removing redundant sequences, the resulted selection of 35 DHAD protein sequences was aligned by ClustalX and then analyzed with MEGA6 using a maximum likelihood statistical method to construct a phylogenetic tree (**Table S1**). The confidence was evaluated with 1000 bootstraps.

Construction of sequence similarity network (SSN)

Sequence similarity network (SSN) for DHAD was generated using the EFI-EST tool (https://efi.igb.illinois.edu/efi-est/). The entire set of DHAD protein sequences from UniProt (InterPro identifier: IPR004404) were used as the input to generate a network. The SSN was generated using an E-value of 15, and was constructed based on an alignment score threshold of 190 that arranges DHADs have a sequence identity of ~60% or greater to be in the same cluster. Cytoscape v.3.7.2 was used for visualization and analysis of the SSN.

Growth inhibition assay of cyanobacteria

To determine the minimal inhibitory concentration (MIC) of inhibitors or BCAAs on *Synechocystis* sp. PCC 6803, 100 µL of cyanobacterial culture in BG-11 medium with an initial OD_{730} of 0.1 were inoculated into each well of 96-well microplate along with serial 2-fold diluted tartronic acid, aspterric acid, BCAAs, or nicosulforon solutions, and then grew under 16 h/8 h light/dark lighting cycle at 26 °C for 10 days. The MIC was determined as the lowest concentration leading to no visible bacterial growth. All experiments were independently performed in triplicate.

The growth inhibition effects of aspterric acid were tested against a panel of microbial pathogens **(Table S2)**. Bacterial and fungal strains were grown at 35 °C medium in LB (Luria-Bertani) liquid and YPD (yeast extract-peptone-dextrose) medium, respectively. Cyanobacteria were cultured in BG-11 medium at 23 °C with continuous air bubbling and under 16 h/8 h light/dark lighting cycle with illumination of 2000–2500 1x during lighting period. Mid-log phase cultures were centrifuged, and the cell pellets were washed and suspended in minimal media (M9 minimal medium for bacteria, synthetic minimal medium for fungus, BG-11 medium for cyanobacteria). The strain solutions were then inoculated in microliter wells containing corresponding minimal media, in the presence of aspterric acid (100 µM for bacteria and fungus, 50 nM for cyanobacteria), or aspterric acid supplemented with leucine (1 mM), isoleucine (1 mM) and valine (1 mM). The plates of bacteria and fungus were incubated at 35 °C for 16-48 h and OD_{600} values were measured using UV/vis microplate spectrophotometer (BioTek). The plates of cyanobacteria were incubated under 16 h/8 h light/dark lighting cycle at 23 °C for 10-20 days and OD_{730} values were recorded. All experiments were independently performed in triplicate.

Table S1. List of selected DHADs for the construction of phylogenetic tree

Strain name	[Fe-S] type	Genbank Accession number	Organism feature
Anabaena	2Fe-2S	WP_026104005.1	cyanobacteria
Nodularia	2Fe-2S	WP_089092735.1	cyanobacteria
Fischerella	2Fe-2S	WP_062242563.1	cyanobacteria
Mastigocoleus testarum	2Fe-2S	WP_027844233.1	cyanobacteria
Oscillatoria	2Fe-2S	WP_015179301.1	cyanobacteria
Lyngbya	2Fe-2S	WP_009784585.1	cyanobacteria
Xenococcus	2Fe-2S	WP_006511494.1	cyanobacteria
Myxosarcina	2Fe-2S	WP_036478690.1	cyanobacteria
Microcystis aeruginosa	2Fe-2S	WP_012265889.1	cyanobacteria
Synechocystis	2Fe-2S	WP_010874288.1	cyanobacteria
Streptococcus pneumoniae	2Fe-2S	WP_000137358.1	bacterium
Arabidopsis thaliana	2Fe-2S	NP_189036.1	plant
Glycine max	2Fe-2S	NP_001276144.1	plant
Schizosaccharomyces pombe	2Fe-2S	NP_593729.1	fungus
Cryptococcus neoformans	2Fe-2S	XP_012053809.1	fungus
Saccharomyces cerevisiae	2Fe-2S	NP_012550.1	fungus
Komagataella phaffii	2Fe-2S	XP_002490591.1	fungus
Candida albicans	2Fe-2S	XP_721948.1	fungus
Mycobacterium tuberculosis	2Fe-2S	WP_003900824.1	bacterium
Sulfolobus acidocaldarius	2Fe-2S	WP_011278523.1	archaeon
Clostridioides difficile	4Fe-4S	WP_011861428.1	bacterium
Methanothermobacter thermautot	4Fe-4S	WP_048061057.1	bacterium
Thermotoga maritima	4Fe-4S	WP_004081337.1	bacterium
Staphylococcus aureus	4Fe-4S	WP_001255791.1	bacterium
Enterococcus	4Fe-4S	WP_008381045.1	bacterium
Streptomyces coelicolor	4Fe-4S	WP_011028925.1	bacterium
Neisseria meningitidis	4Fe-4S	WP_002244135.1	bacterium
Synechococcus elongatus	4Fe-4S	WP_126146830.1	cyanobacteria
Deinococcus radiodurans	4Fe-4S	WP_010887775.1	bacterium
Acinetobacter baumannii	4Fe-4S	KLT83459.1	bacterium
Pseudomonas aeruginosa	4Fe-4S	WP_124212049.1	bacterium
Shewanella oneidensis	4Fe-4S	WP_011074002.1	bacterium
Escherichia coli	4Fe-4S	WP_094888139.1	bacterium
Klebsiella	4Fe-4S	WP_064167055.1	bacterium
Enterobacter	4Fe-4S	WP_109846501.1	bacterium

Table S2. List of strains used in growth inhibition assays

Strain name	[Fe-S] cluster type
Escherichia coli BL21 (DE3)	4Fe-4S
Pseudomonas aeruginosa NRRL B-3059	4Fe-4S
Staphylococcus aureus subsp. Aureus ATCC 29213	4Fe-4S
Candida albicans NRRL YB-3898	2Fe-2S
Synechocystis sp. PCC 6803	2Fe-2S
Anabaena sp. PCC 7120	2Fe-2S
Microcystis aeruginosa NIES 298	2Fe-2S

Table S3. The sequences of primers used in this study.

Primer name	Sequence
SnFw	5'-GATGGATCCATGTCCAACAATCCCAGA-3'
SnRv	5'-GCGCGAATTCTTAGAACAAGTCTATATC-3'
EcFw	5'-GCGGGATCCATGCCTAAGTACCGTTCC-3'
EcRv	5'-GCAGTCGACACCCCCCAGTTTCGATTTATC-3'
MbFw	5'-GGGCATATGATGCCGCAAACCACCGACGAAGCCGCT-3'
MbRv	5'-CAAGAGCTCCTAGCCGCAGACCGCGCCGACCGC-3'
SnC50S-Fw	5'-CACCATTACCCCCAGCAACATGGGCATTAA-3'
SnC50S-Rv	5'-TTAATGCCCATGTTGCTGGGGGTAATGGTG-3'
SnC123S-Fw	5'-TTGGCGATCGGGGGCAGTGATAAGAATATG-3'
SnC123S-Rv	5'-CATATTCTTATCACTGCCCCCGATCGCCAA-3'
SnS473A-Fw	5'-CTTTGCTGGTGGTACCTA-3'
SnS473A-Rv	5'-CACCAGCAAAGCGGCCAT-3'
SnD124L-Fw	5'-TCGGGGGCTGTCTGAAGAATATGCCGG-3'
SnD124L-Rv	5'-CCGGCATATTCTTCAGACAGCCCCCGA-3'
SnD124E-Fw	5'-TCGGGGGCTGTGAAAAGAATATGCCGG-3'
SnD124E-Rv	5'-CCGGCATATTCTTTTCACAGCCCCCGA-3'
MbT495Y-Fw	5'-GGAACCTATGGCCTGTGCGTTGGCCACATC-3'
MbT495Y-Rv	5'- ACGCACAGGCCATAGGTTCCACCGGAGAAC-3'
MbT495H-Fw	5'-GGAACCCACGGCCTGTGCGTTGGCCACATC-3'
MbT495H-Rv	5'-ACGCACAGGCCGTGGGTTCCACCGGAGAAC-3'
pKD-Fw	5'-CAGTGAATGGGGGTAAATGG-3'
pKD-Rv	5'-GCCTGCAGTCTAGACTCGAG-3'
ilvD-sgRNA-Fw	5'-CATGACGCTGGATATCGCGAGTTTTAGAGCTAGAAATAGCAAG-3'
ilvD-sgRNA-Rv	5'-TCGCGATATCCAGCGTCATGGTGCTCAGTATCTCTATCACTGA-3'
pKDsgRNA-Rv	5'-TTTATAACCTCCTTAGAGCTCGA-3'
pKDsgRNA-Fw	5'-CCAATTGTCCATATTGCATCA-3'
Km-Fw	5'-CCGTCCCATTTACGAGACAGACACTGGGAGTAAATAAAGTATGAGCCATATTCAACGGGA-3'
Km-Rv	5'-CCTTCCGGAGCACCGGACAGGGGTTGCGAGTCAGCCATTATTAGAAAAACTCATCGAGCA-3'
Sn-ilvD-Fw	5'-CATATGTCCAACAATCCCAG-3'
Sn-ilvD-Rv	5'-CTCGAGTTAGAACAAGTCTA-3'

Table S4. Data collection, phasing, and refinement statistics

Diffraction Source	21-ID-F (0.9787 Å)
Resolution range (Å)[#]	36.04 - 2.33 (2.413 - 2.33)
Space group	P 1 21 1
Unit cell (Å)	*a* = 79.79, *b* = 74.26, *c* = 80.68
(°)	*α* = *γ* = 90, *β* = 90.15
Total reflections	79549 (7524)
Unique reflections	40231 (3829)
Multiplicity	2.0 (2.0)
Completeness (%)	99.33 (95.25)
Mean I/sigma (I)	11.59 (2.24)
Wilson B-factor	30.59
R-merge	0.05452 (0.3724)
R-meas	0.0771 (0.5267)
R-pim	0.05452 (0.3724)
$CC_{1/2}$[†]	0.997 (0.73)
CC*	0.999 (0.919)
Reflections used in refinement	40224 (3828)
Reflections used for R-free	2153 (231)
R_{work}[†]	0.1724 (0.2279)
R_{free}[†]	0.2249 (0.2964)
CC_{work}	0.964 (0.875)
CC_{free}	0.933 (0.796)
Number of non-hydrogen atoms	7279
macromolecules	7023
solvent	256
Protein residues	971
RMS bonds (Å)	0.009
RMS angles (°)	1.32
Ramachandran favored (%)	96.88
Ramachandran allowed (%)	3.12
Ramachandran outliers (%)	0.00
Rotamer outliers (%)	0.00
Clashscore	5.35
Average B-factor (Å^2)	36.90
macromolecules	37.00
solvent	34.15

[#]Highest resolution shell is shown in parenthesis. [†] $CC_{1/2} = \sum(x - \langle x \rangle)\,(y - \langle y \rangle) / \sqrt{\sum(x - \langle x \rangle)^2 \sum(y - \langle y \rangle)^2}$. *R-factor* $= \sum_{hkl} \big| |F_{obs}| - |F_{calc}| \big| \,/\, \sum_{hkl} |F_{obs}|$, where F_{obs} and F_{calc} are measured and calculated structure factors, respectively. R_{free} calculated from 5% of the reflections that were selected randomly and omitted during refinement.

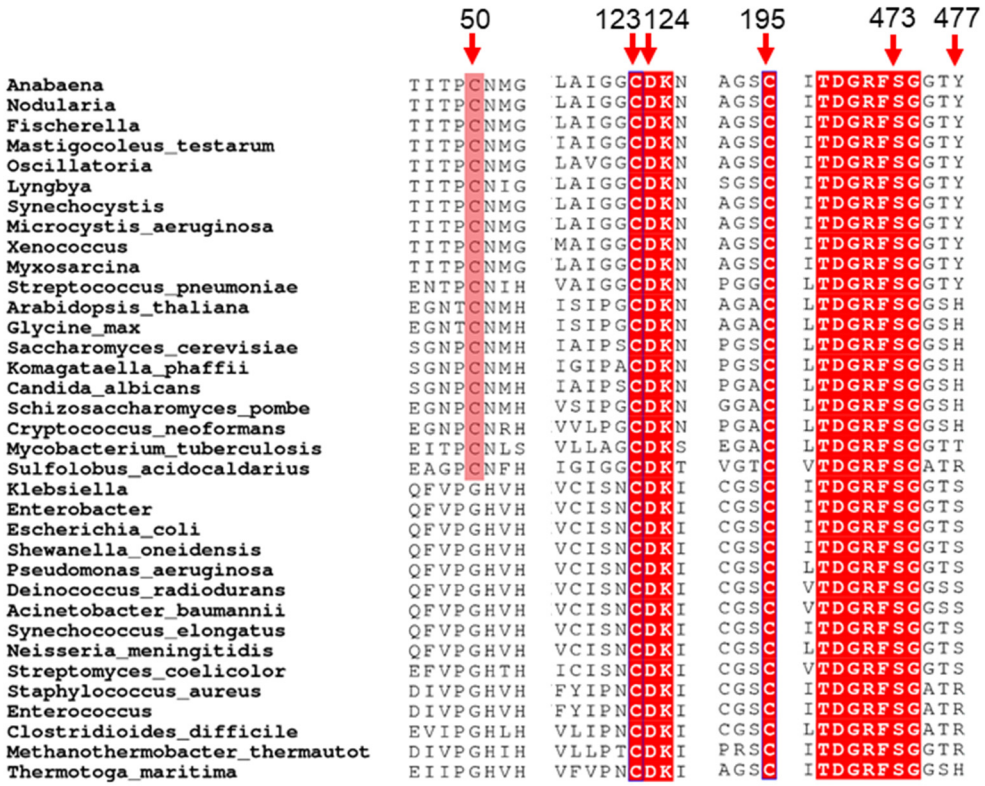

Fig. S1. Key conserved residues among 35 selected DHADs of bacteria, fungi, and plants. Residues are numbered from the SnDHAD sequence. Residues involved in the binding of [Fe-S] clusters, catalysis and oxygen stability are indicated with red arrows.

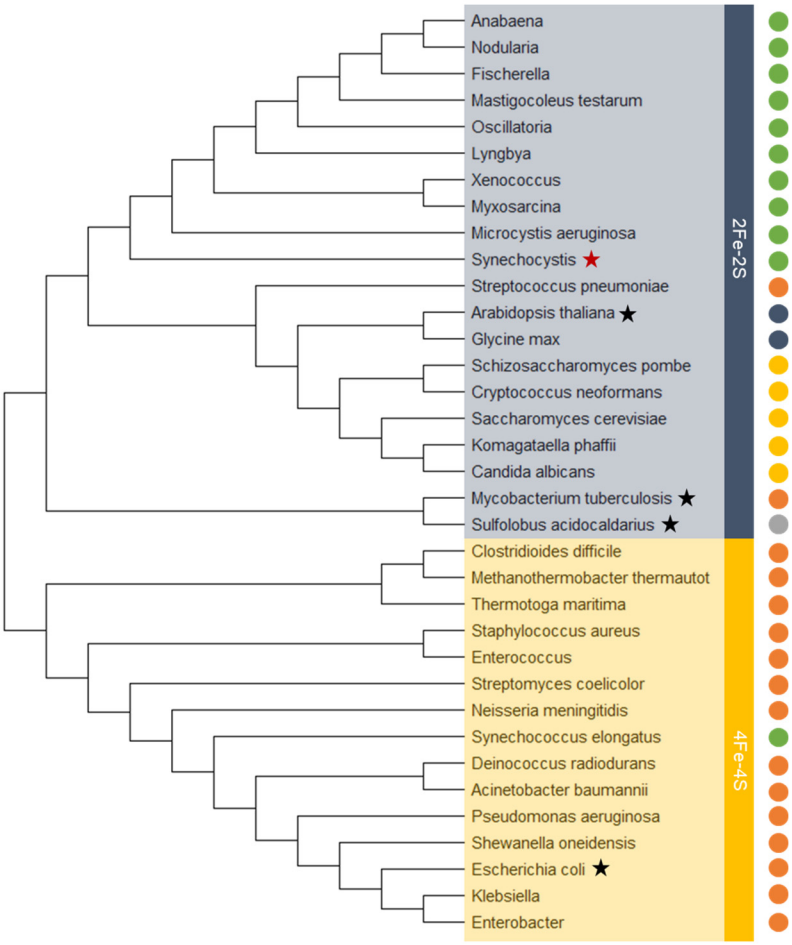

Fig. S2. Phylogenetic analysis of 35 selected DHADs revealed two major clades, one for enzymes with a [2Fe-2S] cluster (blue) and the other with a [4Fe-4S] cluster (yellow). Circles in green, dark blue, grey, yellow, and orange indicate cyanobacteria, plants, archaeon, fungi, and other bacteria. Stars indicate proteins have been characterized.

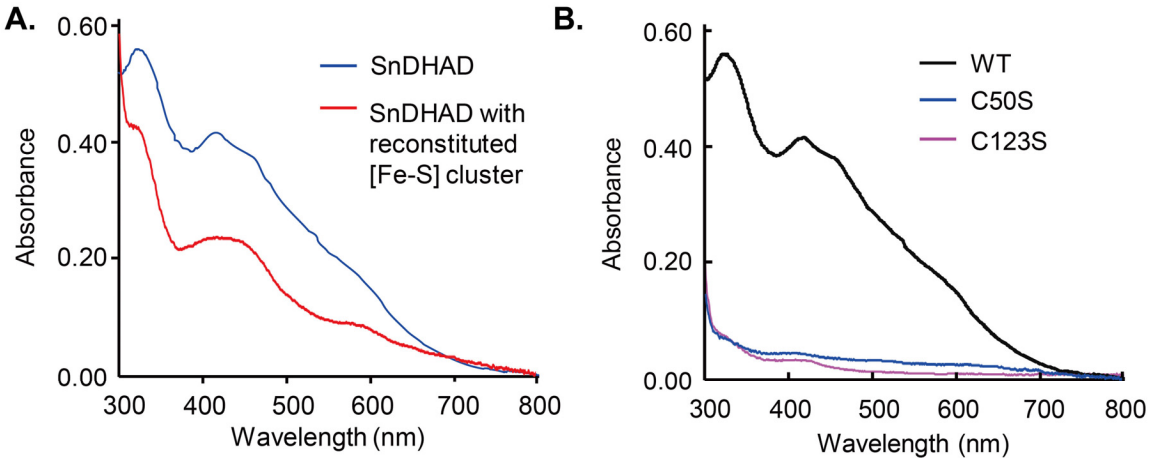

Fig. S3. UV-vis spectral analysis of as-purified SnDHAD, reconstituted enzyme, and C50S and C123S mutants.

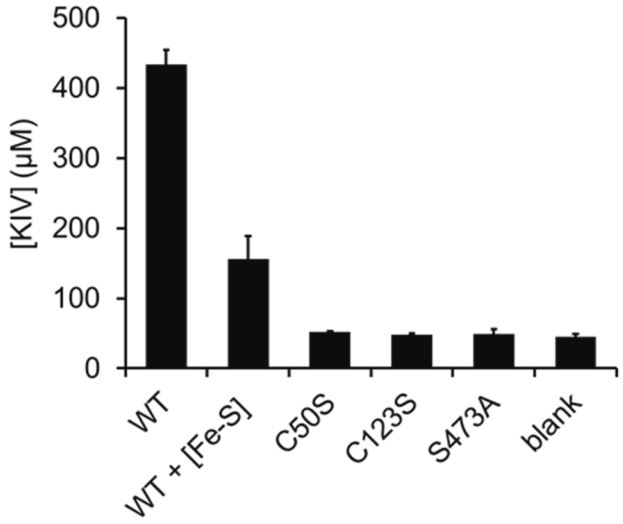

Fig. S4. Absolute amounts of KIV produced from 2*R*-DHIV (1mM) in the reactions of SnDHAD and its mutants. The reactions contained 1 mM substrate and 0.25 μM enzyme and were incubated at room temperature for 30 min. Produced KIV was derivatized with DNPH for HPLC-based quantification. Data represent means ± S.D. of at least three independently repeated experiments.

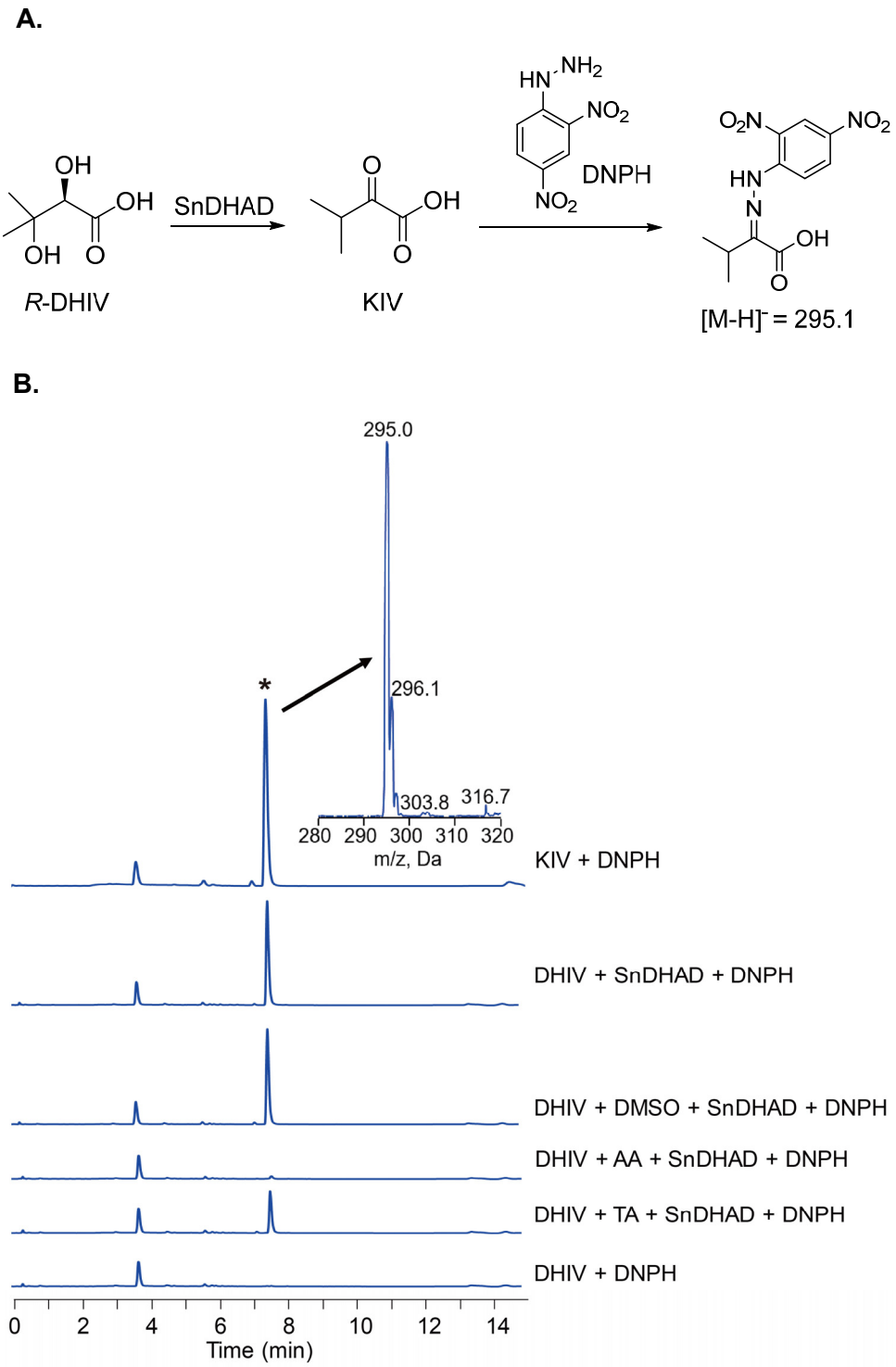

Fig. S5. LC-MS analysis of SnDHAD reactions after DNPH derivatization of synthesized KIV. **A:** Scheme of DNPH derivatization of KIV produced from DHIV by SnDHAD. **B:** LC traces of enzymatic and control reactions after derivatization. * indicates the KIV-DNPH adduct and inlet shows the MS spectrum. AA at 50 nM completely inhibited the enzyme reaction, while TA at 0.5 mM achieved a partial inhibition.

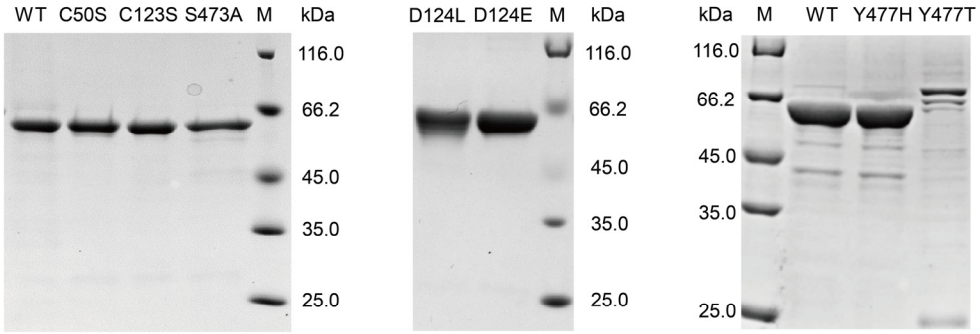

Fig. S6. SDS-PAGE of purified recombinant wild type (WT) SnDHAD and its mutants. All enzymes except SnDHAD Y477T showed expected molecular weights.

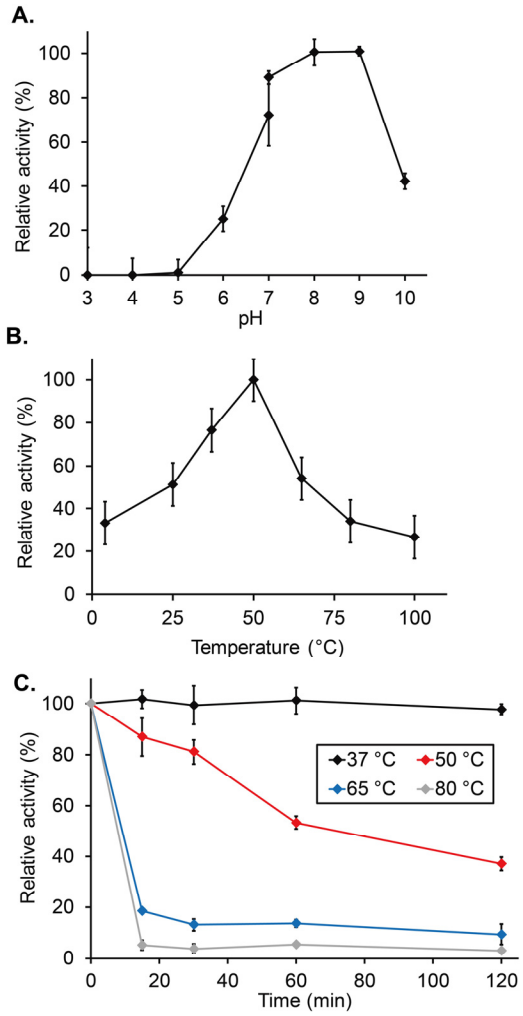

Fig. S7. Optimal conditions of SnDHAD reaction. **A:** SnDHAD showed the highest activity in the buffer with pH of 8 to 9. **B:** SnDHAD had the highest activity at 50 °C. **C:** Thermostability of SnDHAD was determined at 37, 50, 65, and 80 °C. The enzyme was incubated at the indicated temperatures for 15 min and the residual activity was then determined. Data represent means ± S.D. of at least three independently repeated experiments.

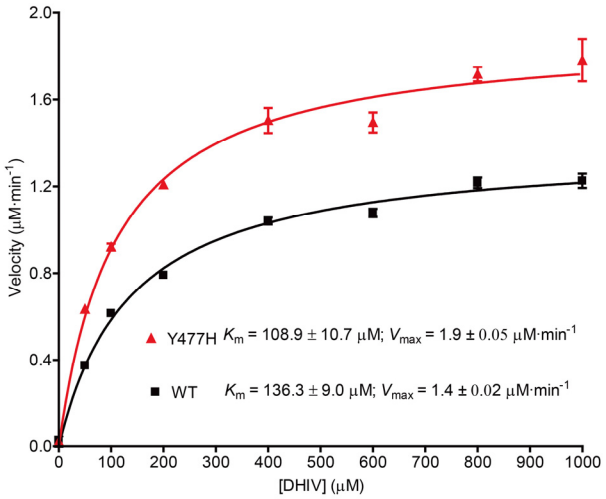

Fig. S8. Michaelis-Menten plots showing the kinetic performance of as-purified SnDHAD wild type (WT) and Y477H mutant. This analysis determined the calculated K_m and V_{max} values of 136.3 ± 9.0 μM and 1.4 ± 0.02 μM·min^{-1}, respectively, for WT and 108.9 ± 10.7 μM and 1.9 ± 0.05 μM·min^{-1} , respectively, for the Y477H mutant. Data represent means ± S.D. of at least three independently repeated experiments.

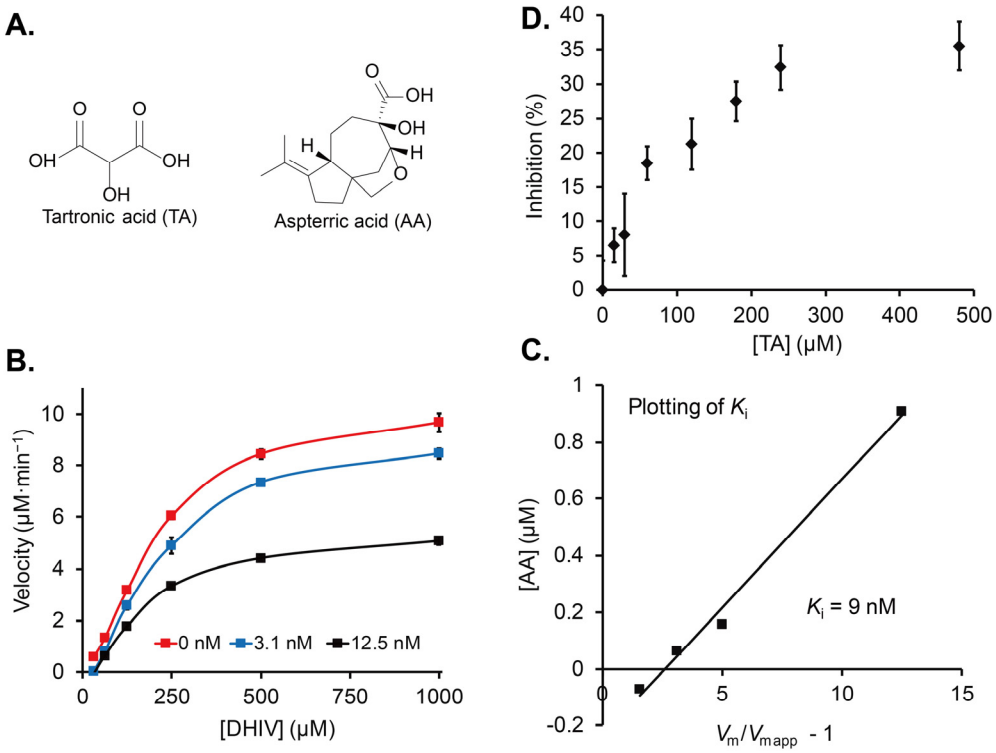

Fig. S9. AA potently inhibits SnDHAD reaction. **A:** Chemical structures of TA and AA. **B**: Michaelis-Menten plots of SnDHAD reactions with 0, 3.1, and 12.5 nM of AA. **C:** The Lineweaver-Burk plot showed a noncompetitive inhibition, with a K_i of 9 nM. **D:** SnDHAD reaction was inhibited to about 35% with up to 0.5 mM TA. Data represent means ± S.D. of at least three independently repeated experiments.

A.

Enzymes	AtDHAD	MbDHAD	SnDHAD
AtDHAD		46%	51%
MbDHAD	46%		51%
SnDHAD	51%	51%	

B.

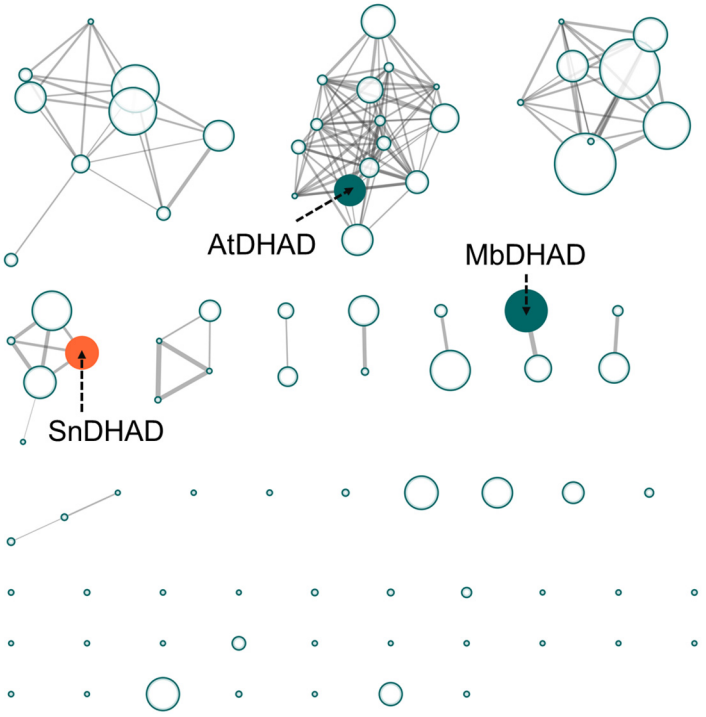

Fig. S10. A: Amino acid identities of AtDHAD, MbDHAD, and SnDHAD. **B:** Sequence similarity network (SSN) for DHADs constructed by EFI. Nodes represent proteins with ~60% or greater sequence identity, and the size of nodes correlate to the cluster size. Two nodes that contain structurally characterized DHADs are highlighted in green, MbDHAD (PDB: 6OVT) and AtDHAD (PDB: 5ZE4). The node containing SnDHAD (this study, PDB: 6NTE) is colored in orange.

A.

AA	250 nM	125 nM	62.5 nM	31.25 nM	15.63 nM	7.81 nM	3.90 nM	2.0 nM	1.0 nM	0 nM
AA + B	250 nM	125 nM	62.5 nM	31.25 nM	15.63 nM	7.81 nM	3.90 nM	2.0 nM	1.0 nM	0 nM
TA	250 µM	125 µM	62.5 µM	31.25 µM	15.63 µM	7.81 µM	3.90 µM	2.0 µM	1.0 µM	0 µM
TA + B	250 µM	125 µM	62.5 µM	31.25 µM	15.63 µM	7.81 µM	3.90 µM	2.0 µM	1.0 µM	0 µM

B.

0.073	0.064	0.07	0.333	0.694	0.726	0.771	0.814	0.81	0.831
0.219	0.402	0.539	0.667	0.73	0.775	0.83	0.81	0.834	0.834
0.099	0.498	0.818	0.803	0.787	0.824	0.778	0.741	0.789	0.774
0.386	0.708	0.78	0.757	0.763	0.802	0.799	0.762	0.776	0.756

Fig. S11. The growth inhibition of *Synechocystis* sp. PCC 6803 by serial concentrations of AA and TA in the presence and absence of 0.05 mM BCAAs (B). **A:** Concentrations of AA and TA with or without BCAAs in different wells of one microplate. **B:** Cell optical densities at 730 nm were determined in different wells.

A.

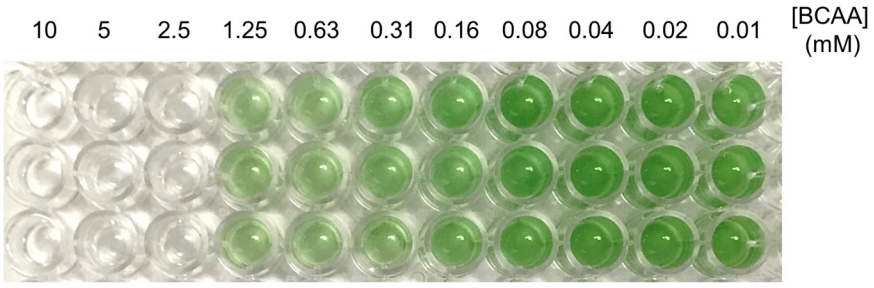

B.

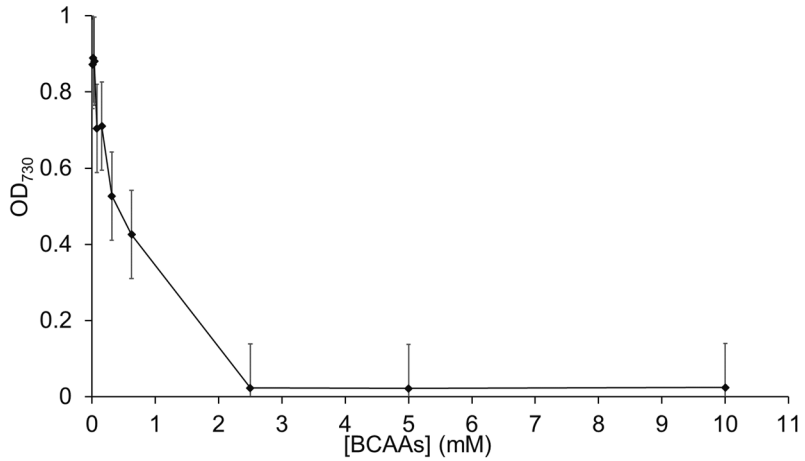

Fig. S12. BCAAs inhibit the growth of *Synechocystis* sp. PCC6803 in a dose-dependent manner. **A:** MIC of BCAAs was determined as 2.5 mM using the standard 2-fold serial dilution approach. **B:** Cell optical densities at 730 nm were plotted against serial BCAAs concentrations. Data represent means ± S.D. of at least three independently repeated experiments.

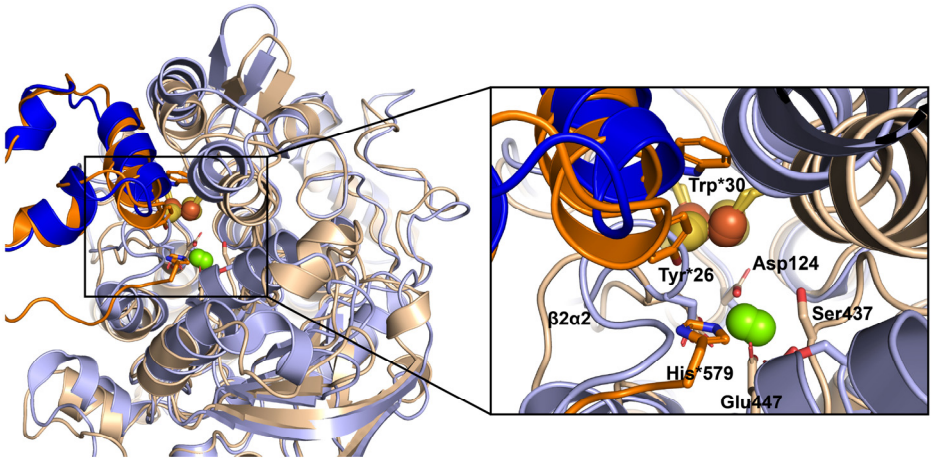

Fig. S13. The active sites of ArDHT (PDB: 5J84) in oranges and AtDHAD (PDB: 5ZE4) in blues are overlaid, highlighting the residues in the *N*-terminal region and the *C*-terminal histidine that extend into the active site. No residues in the *N*-terminal domain of DHAD extend into the active site. In fact, the β2α2 loop of DHAD replaces these residues that extend into the active site of ArDHT.

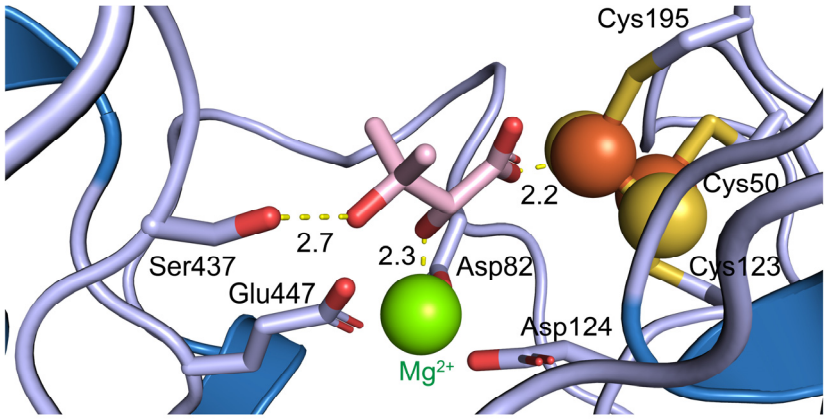

Fig. S14. SnDHAD with DHIV modelled showing key interatomic distances, in Angstroms. DHIV interacts with both the 2Fe-2S cluster as well as Mg^{2+}. The Mg^{2+} is coordinated by Asp82, Asp124, and Glu447. The 2Fe-2S cluster is coordinated by Cys50, Cys123, and Cys 195. DHIV was modelled using Schrodinger Glide. The 1C carboxyl is 2.2 Å away from the unoccupied iron of the 2Fe-2S cluster. The 2C hydroxyl of DHIV is 2.3 Å away from the Mg^{2+}. The 3C hydroxyl is 2.7 Å away from Ser437, which is positioned to protonate the leaving group.

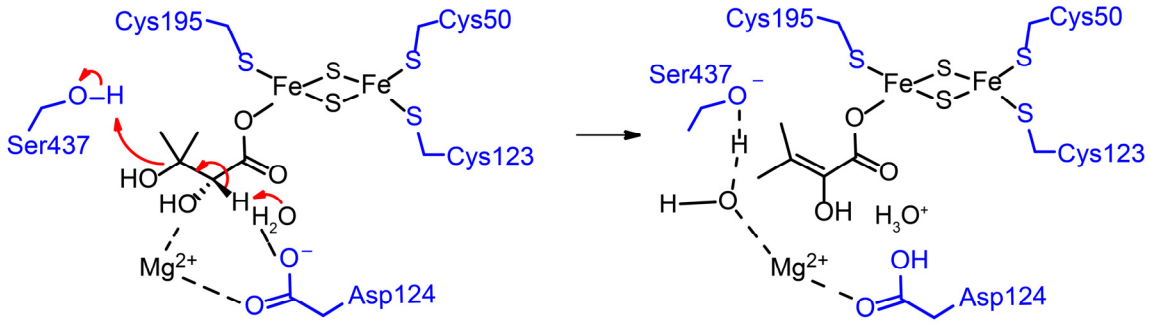

Fig. S15. A proposed reaction mechanism of SnDHAD with a new binding mode of DHIV.

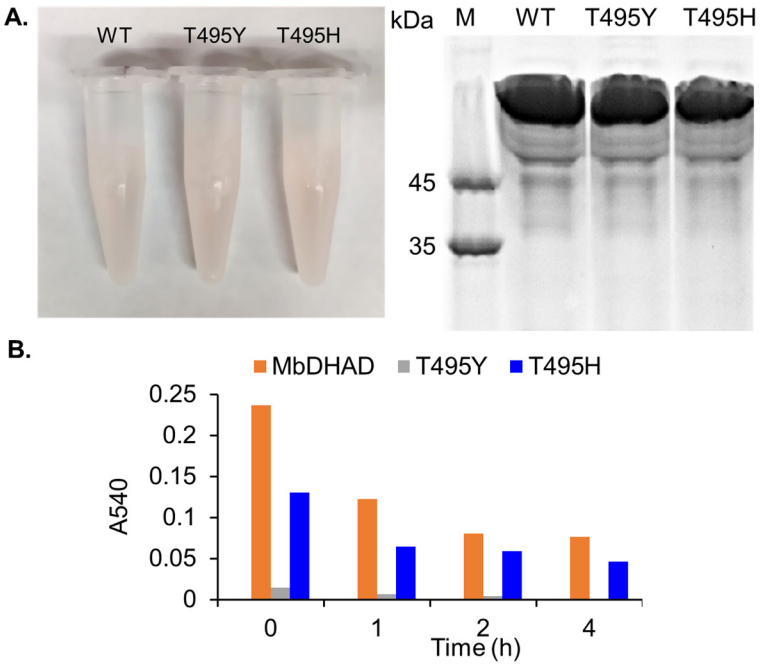

Fig. S16. A: As-purified MbDHAD, T495Y and T495H were brown and showed expected molecular weight in SDS-PAGE analysis. **B:** MbDHAD, T495Y and T495H decreased their catalytic activity along with the increased air exposure for 0, 1, 2, 3, and 4 h. The reactions were set up under the same conditions as SnDHAD, with 0.25 μM enzyme and 1 mM substrate in the room temperature reactions for 30 min. Data represent means ± S.D. of three independently repeated experiments.

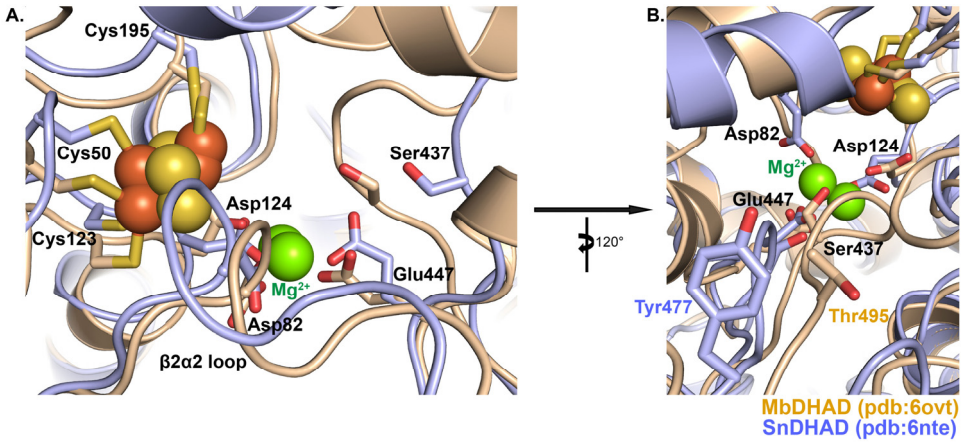

Fig. S17. Structural insights of SnDHAD oxygen stability. **A**: The overlaid active sites of SnDHAD in blue and MbDHAD (PDB: 60VT) in orange, highlighting the loop containing the catalytic serine (Ser437 in SnDHAD). This loop is about 5Å closer to the 2Fe-2S cluster in MbDHAD relative to SnDHAD. The MbDHAD conformation could represent a "closed" state, while the SnDHAD conformation represents an "open" state. **B:** An alternate view of the active site, highlighting the Tyr477 and Thr495 that sit above the binding pocket, in the protein tunnel that leads to the active site. Oxygen resistance could be due to the Tyr477 in SnDHAD that covers the binding site, occluding oxygen. MbDHAD does not contain an aromatic amino acid at this position and instead contains a threonine, which would not occlude oxygen as well as tyrosine.

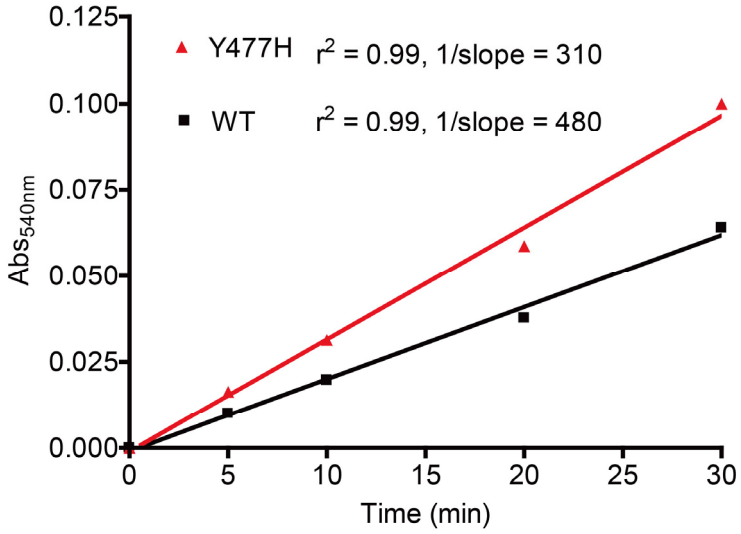

Fig. S18. Conversion rates of as-purified SnDHAD wild type and Y477H mutants. The reactions contained 0.05 μM enzyme, 1 mM DTT, 10 mM $MgCl_2$ and 1 mM 2*R*-DHIV in 50 mM Tris-Cl, pH 8.0. The reactions were incubated aerobically at room temperature and 100 μL of reaction solutions were taken out at 0, 5, 10, 20, and 30 min to determine KIV concentrations at 540 nm after derivatization with DNPH. Data represent means ± S.D. of three independently repeated experiments and were fitted to linear regression by Prism 4.0.

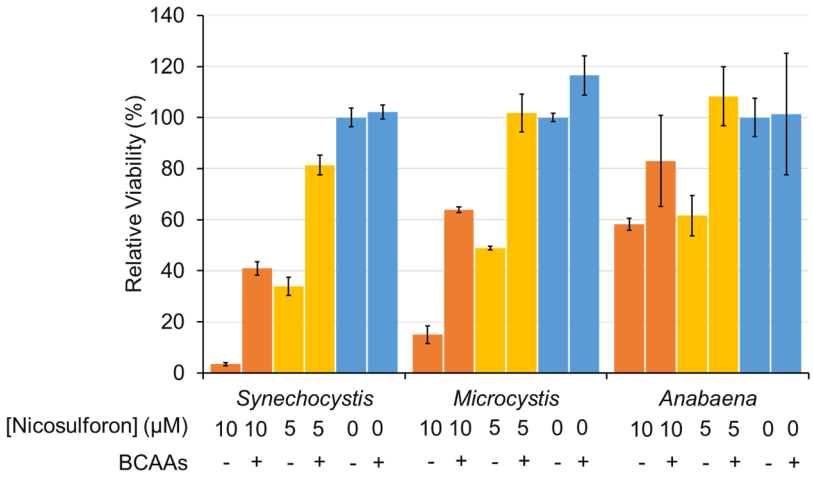

Fig. S19. Growth inhibition of *Synechocystis* sp. PCC 6803, *Microcystis aeruginosa* NIES 298 and *Anabaena* sp. PCC 7120 by serial 2-fold dilution of nicosulforon in BG-11 medium with or without 0.05 mM BCAAs. Data represent means ± S.D. of at least three independently repeated experiments.

A.

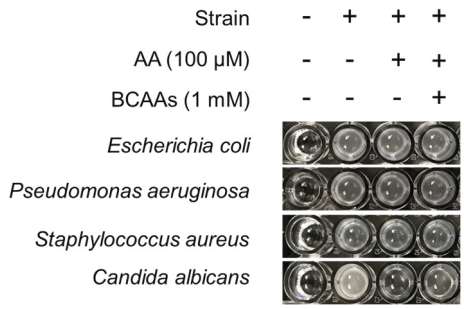

B.

Strain	-	+	+	+
AA (100 μM)	-	-	+	+
BCAAs (1 mM)	-	-	-	+
Escherichia coli	0.041 ± 0.002	0.246 ± 0.004	0.255 ± 0.001	0.241 ± 0.005
Pseudomonas aeruginosa	0.044 ± 0.001	0.238 ± 0.009	0.244 ± 0.003	0.262 ± 0.014
Staphylococcus aureus	0.040 ± 0.001	0.228 ± 0.036	0.210 ± 0.012	0.226 ± 0.012
Candida albicans	0.045 ± 0.004	0.834 ± 0.023	0.299 ± 0.010	0.416 ± 0.055

Fig. S20. Growth inhibition of selected bacterial pathogens and the fungal pathogen *Candida albicans* by 100 μM of AA. **A:** A picture of microbial pathogen growth in minimal media with indicated AA and BCAAs in 96-well plate. **B:** Optical densities of microbial pathogens under different treatments were determined at 600 nm. Data represent means ± S. D. of at least three independent experiments.

References:

1. Jeitner, T. M. (2014) Optimized ferrozine-based assay for dissolved iron, *Anal Biochem 454*, 36-37.
2. Reisch, C. R., and Prather, K. L. (2015) The no-SCAR (Scarless Cas9 Assisted Recombineering) system for genome editing in *Escherichia coli*, *Sci Rep 5*, 15096.
3. Kabsch, W. (2010) Xds, *Acta Crystallogr D 66*, 125-132.
4. Stein, N. (2008) CHAINSAW: a program for mutating pdb files used as templates in molecular replacement, *J Appl Crystallogr 41*, 641-643.
5. Cowtan, K. (2006) The Buccaneer software for automated model building. 1. Tracing protein chains, *Acta Crystallogr D 62*, 1002-1011.
6. Adams, P. D., Afonine, P. V., Bunkoczi, G., Chen, V. B., Davis, I. W., Echols, N., Headd, J. J., Hung, L. W., Kapral, G. J., Grosse-Kunstleve, R. W., McCoy, A. J., Moriarty, N. W., Oeffner, R., Read, R. J., Richardson, D. C., Richardson, J. S., Terwilliger, T. C., and Zwart, P. H. (2010) PHENIX: a comprehensive Python-based system for macromolecular structure solution, *Acta Crystallogr D 66*, 213-221.
7. Song, Y., DiMaio, F., Wang, R. Y., Kim, D., Miles, C., Brunette, T., Thompson, J., and Baker, D. (2013) High-resolution comparative modeling with RosettaCM, *Structure 21*, 1735-1742.
8. Sievers, F., Wilm, A., Dineen, D., Gibson, T. J., Karplus, K., Li, W. Z., Lopez, R., McWilliam, H., Remmert, M., Soding, J., Thompson, J. D., and Higgins, D. G. (2011) Fast, scalable generation of high-quality protein multiple sequence alignments using Clustal Omega, *Mol Syst Biol 7*, 539. doi: 10.1038/msb.2011.75.
9. Fleishman, S. J., Leaver-Fay, A., Corn, J. E., Strauch, E. M., Khare, S. D., Koga, N., Ashworth, J., Murphy, P., Richter, F., Lemmon, G., Meiler, J., and Baker, D. (2011) RosettaScripts: a scripting language interface to the Rosetta macromolecular modeling suite, *PLoS One 6*, e20161.